Journal of Statistical Physics, Vol. 71, Nos. 3/4, 1993

Critical Behavior of Self-Avoiding Walks on Fractals

Fábio D. A. Aarão Reis[1] and R. Riera[1]

Received December 3, 1991; final July 30, 1992

Using a new graph counting technique suitable for self-similar fractals, exact 18th-order series expansions for SAWs on some Sierpinski carpets are generated. From them, the critical fugacity x_c and critical exponents ν_{SAW} and γ_{SAW} are obtained. The results show a linear dependence of the critical fugacity with the average number of bonds per site of the lattices studied. We find for some carpets with low lacunarity that $\nu_{\mathrm{SAW}} < 0.75$, thus violating the relation $\nu_{\mathrm{SAW}}(\text{fractal}) > \nu_{\mathrm{SAW}}(d)$ for SAWs on the fractals which are embedded in a d-dimensional Euclidean space.

KEY WORDS: Self-avoiding walks; fractals; series expansion.

1. INTRODUCTION

The study of the critical behavior of self-avoiding walks (SAWs) on Euclidean lattices has three main theoretical approaches. On one hand, there are phenomenological theories or Flory-like approximations, where SAWs model the excluded-volume effect in polymer chains,[1,2] and on the other hand, series expansions for the geometrical properties of the walk[3,4] and field-theoretical approaches.[5,6]

During the last decade, much effort has been made in the study of the critical behavior of SAWs on fractals. Some exact results were presented for the case of finitely ramified fractals,[7] such as Koch curves or Sierpinski gaskets.[8]

There also have been numerical studies of SAWs on percolation clusters,[9] but the main theoretical effort on SAWs on general fractal lattices is based on the Flory approach.

[1] Departamento de Física, Pontifícia Universidade Católica do Rio de Janeiro, 22452 Rio de Janeiro RJ, Brazil.

The first attempt to generalize Flory theory to fractal lattices was made by Kremer[10] for the exponent that scales the average end-to-end distance R with N, the number of steps of the walks ($R \sim N^{\nu_{SAW}}$):

$$\nu_k = 3/(2 + D_f) \tag{1}$$

with D_f the fractal dimension of the lattice.[7]

As D_f does not completely characterize the fractal geometry, other proposals were made[8, 11, 12] which relate ν_{SAW} to other geometrical parameters of the lattice as well as to the problem of a random walk on the same lattice. Although the authors give phenomenological justifications for their expressions, the final validity of the proposals demands comparisons with more reliable theoretical estimates.

For finitely ramified fractals the results from the above Flory generalizations improve the estimate (1), yet present an average deviation of 5% from the available exact results, while for infinitely ramified fractals, those estimates of ν_{SAW} are uncertain due to their dependence on geometrical parameters that are not precisely known. Numerical simulations are constrained to finite lattices.[13]

In this paper, we present results for the critical behavior of SAWs on a family of infinitely ramified fractals called Sierpinski carpets, based on the series expansion method. The series obtained are exact order by order in the expansion parameter for the infinite lattice. As in Euclidean lattices, this approach provides reliable estimates for critical parameters and exponents whose accuracy can be improved in a systematic way by increasing the order of the series.

From our results, we test the validity of estimates previously obtained in the literature from approximate methods.

In the next section we review a technique of graph counting on regular fractals[14] that provides the series expansion method for SAWs on these general lattices. Subsequently in Section 3 we present results from series up to 18th order for some Sierpinski carpets. Section 4 comprises a discussion and conclusion.

2. GRAPH COUNTING ON REGULAR FRACTALS

Here, we consider regular fractals formed by a deterministic rule of construction in which a primitive initiator is divided into subunits and reproduced iteratively within each subunit. Figure 1 illustrates the case of Sierpinski carpets where the initiator is a square divided into subsquares of length scale b times smaller. Among the b^2 subsquares formed, m are non-reproducible (lacunas) for the next iterations. After l iterations, the lattice

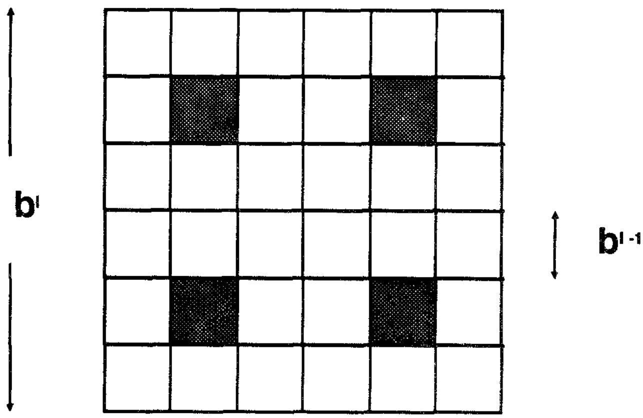

Fig. 1. Sierpinski carpet at the lth stage of construction. Here $b=6$, $m=4$. The dashed subsquares are lacunas. Each open subsquare is a reproduction of the full lattice after $l-1$ iterations of the rule of construction, which is given by the first iteration.

is said to be at the lth stage. The fractal lattice is obtained in the limit $l\to\infty$. Figure 1 shows an l-stage Sierpinski carpet: it has as subunits copies of the lattice at the previous $(l-1)$th stage. These copies have the same spatial arrangement as the subunits of the initiator (first stage). The fractal thus constructed has fractal dimension $D_f=\ln(b^2-m)/\ln b$.[7]

SAWs are represented by graphs on the lattice formed by connected bonds without self-intersections and having two endpoints. Each different geometrical form defines a type of graph. Our aim is to count the number of embeddings of each type of SAW in the lattice at each stage. We consider the bonds at the borders as well as free boundary conditions.

In what follows we will describe the method for the Sierpinski carpets with lacunas symmetrically distributed with respect to the center of the initial square and not at the border. However, the method can be easily extended to other carpets or any other regular fractal.

The number $G(l)$ of embeddings of a certain type of SAW in the lattice at stage l is given by[14]

$$G(l)=(b^2-m)\,G(l-1)+H(l-1) \tag{2a}$$

with

$$H(l-1)=H_1(l-1)+H_2(l-1)=C_1 b^{l-1}+C_2 \tag{2b}$$

In (2a), the first term represents the number of SAWs that can be embedded in each one of the (b^2-m) copies of the $(l-1)$th stage at lattice stage l (see Fig. 1). The terms $H_1(l-1)$ and $H_2(l-1)$ represent the total number of configurations that cross two or more such copies, respectively. In (2b), constants C_1 and C_2 depend only on properties of the graph at the minimal stage l_0 that embeds it. A detailed derivation of Eq. (2b) is shown in the Appendix.

Iterating (2) up to the stage l_0 gives

$$G(l) = A(b^2 - m)^l + Bb^l + C \tag{3}$$

with constants A, B, and C depending on the constants in (2).

Equation (3) is valid for all types of connected graphs[14] and, in particular, for the number of sites S (graphs with zero bonds):

$$S(l) = A_1(b^2 - m)^l + B_1 b^l + C_1 \tag{4}$$

From (3) and (4) we obtain the density of each type of SAW in the fractal lattice:

$$\rho_{\mathrm{SAW}} = \lim_{l \to \infty} \frac{G(l)}{S(l)} = \frac{A}{A_1} \tag{5}$$

With this method it is also possible to obtain several geometrical parameters of the fractal lattice. For instance, from the number of graphs with one bond at each stage $G_1(l)$ and the number of sites $S(l)$ we are able to calculate the average coordination number of the fractal lattices, which is twice the average number of bonds per site:

$$q = \lim_{l \to \infty} \frac{G_1(l)}{S(l)} \tag{6}$$

An important geometrical parameter for characterizing the critical behavior on fractals is lacunarity,[7] which represents the degree of homogeneity of the fractals.[15] The expressions proposed in the literature to measure lacunarity for carpets[15,16] have so far been calculated only for the first states of the lattices. Our method allows the calculation of these expressions in the $l \to \infty$ stage.

3. RESULTS FOR SIERPINSKI CARPETS

Consider the series expansions for the two generating functions

$$C(x) = \sum_{n=0}^{\infty} C_n x^n \tag{7a}$$

$$R(x) = \sum_{n=1}^{\infty} \langle R_n^2 \rangle x^{n-1} \tag{7b}$$

where x is the step fugacity, C_n is the number of n-step SAWs per site, and $\langle R_n^2 \rangle$ is the mean-square end-to-end distance of n-step SAWs per site.

The generating functions (7) have, respectively, the critical behavior[2]

$$C(x) \sim (x_c - x)^{-\gamma_{\mathrm{SAW}}} \tag{8a}$$

$$R(x) \sim (1 - x)^{-(2\nu_{\mathrm{SAW}} + 1)} \tag{8b}$$

The coefficients C_n in (7a) may be obtained from (5), and $\langle R_n^2 \rangle$ in (7b) from (5) and the end-to-end distance for each type of SAW.

The procedure used to obtain C_n (and R_n^2) for each particular fractal lattice is as follows:

(i) generation by computer of all types (different geometrical forms) of n-step SAWs on a square lattice. For each type,

(ii) consider the minimal stage l_0 of the fractal lattice that embeds it and compute exactly the total number of possible embeddings of the SAW at this stage [this gives $G(l_0)$; see text]

(iii) consider two neighboring l_0-stage reproductions and compute the total number of possible embeddings that cross the intersection between then [this gives the contribution to $H_1(l_0)$; see text]

(iv) consider more than two neighboring l_0-stage reproductions (for the Sierpinski carpets we have just to consider three or four reproductions) and compute the total number of possible embeddings that cross two or more intersections between them (this gives the contribution to $H_2(l_0)$; see text]

(v) from (iii) and (iv), according (A.3)–(A.5), obtain $H(l-1)$ in Eq. (2)

(vi) iterating (2) up to stage l_0 and using (ii), obtain constants A, B, C in Eq. (3)

(vii) finally, C_n is obtained from (5) by adding the contributions of all types of n-step SAWs.

To prevent errors, we have checked the results for SAWs up to 11 steps, rederiving constants A, B, and C in Eq. (3) from the interaction of Eq. (2) up to the $(l_0 + 1)$ stage and computing directly (ii)–(v) for this stage.

Another check for small SAWs was done by computing directly the number of embeddings at three consecutives stages of construction of the fractal lattice. From these results and assuming Eq. (3), the constants A, B, and C were also confirmed.

We have performed the exact calculations of the coefficients C_n and $\langle R_n^2 \rangle$ for some Sierpinski carpets. Figure 2 shows the first stage of these lattices. They have respectively parameters $b = 5$, $m = 1$ (lattice 1); $b = 7$,

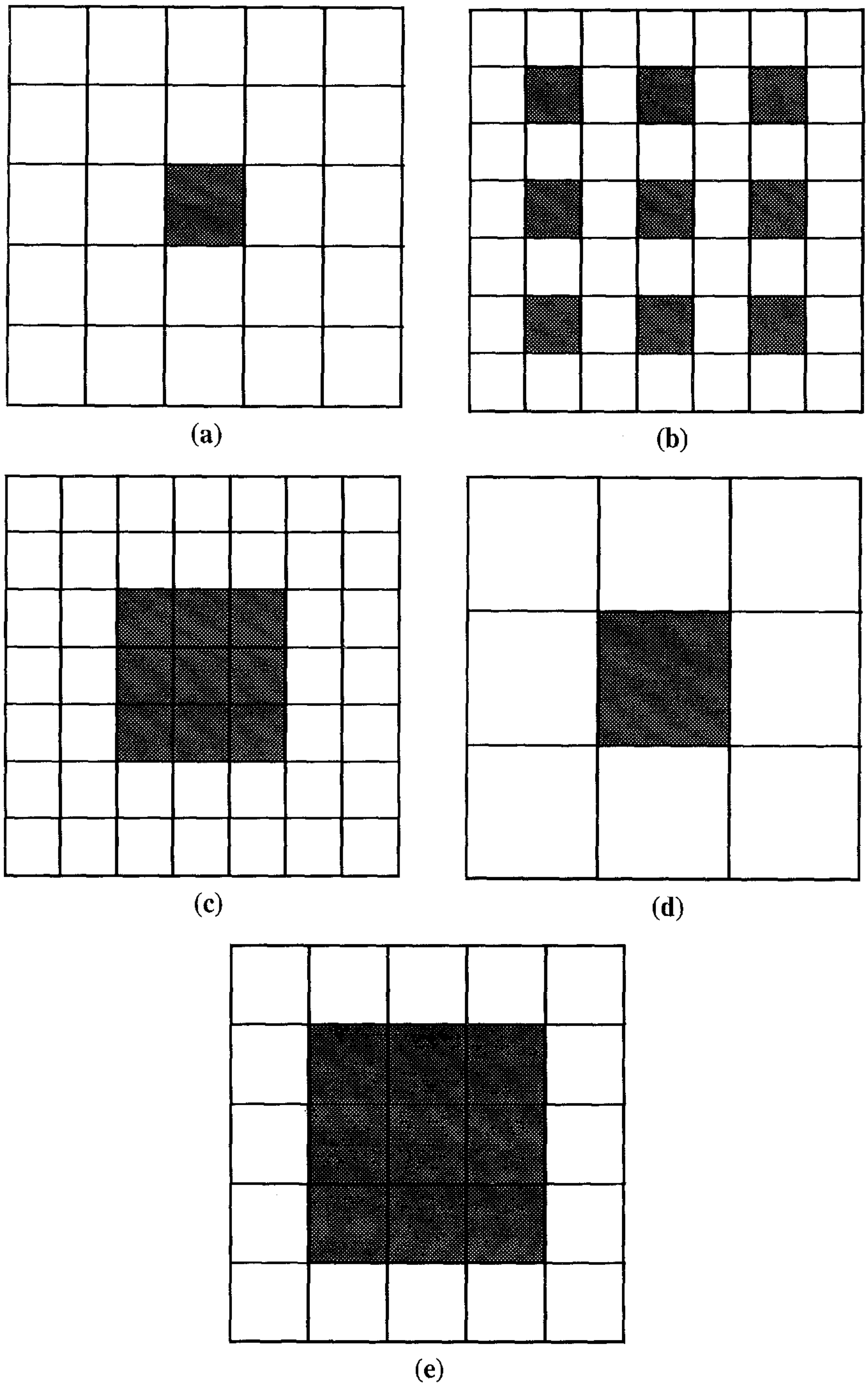

Fig. 2. Initiators of Sierpinski carpets: (a) $b=5$, $m=1$; (b, c) $b=7$, $m=9$; (d) $b=3$, $m=1$; (e) $b=5$, $m=9$.

$m = 9$ (lattices 2 and 3); $b = 3$, $m = 1$ (lattice 4); and $b = 5$, $m = 9$ (lattice 5). Lattices 2 and 3 have the same fractal dimension, but lattice 2 has a lower lacunarity, or a more uniform spatial distribution of lacunas.[15]

Tables I–V show the coefficients C_n and $\rho_n = C_n\langle R_n^2\rangle$ for lattices 1–5, respectively.

The resulting 18th-order series (7) were analyzed by usual D log Padé approximants[17] in order to fit (8).

In Tables VI–X we show the poles and residues of Padé approximants to the logarithmic derivative of the SAW series (7a)[17] that provides estimates for the critical fugacity x_c and exponent γ_{SAW} in (8a), for lattices 1–5, respectively. Analogously, in Tables XI–XV, we show the value of D log Padé approximants of the SAW series (7b) that provides estimates for $(2\gamma_{\text{SAW}} + 1)$ in (8b) at the biased critical value $x^* = 1$.

Final estimates of x_c, γ_{SAW} and ν_{SAW} are obtained by considering the last $M = 9$ estimates of the $[N_i/D_i]$ approximants shown in Tables VI–XV and using the standard procedure for the error assessment.[18]

Table XVI shows the results for critical parameters x_c, critical exponents ν_{SAW} and γ_{SAW}, together with D_f and the average number of bonds per site q (6) for each lattice. For comparison, we include the results for the square lattice from an 18th-order series expansion of (7) and the same criteria for the estimates.

Table I. Coefficients $C(x)$ and $R(x)$ for SAWs on the Sierpinski Carpet with $b = 5$, $m = 1$ (see Fig. 2a)

n	C_n	ρ_n
1	115/29	115/29
2	342/29	912/29
3	48893/1392	222461/1392
4	22461/232	473666/696
5	63337/232	1813039/696
6	1035941/1392	6496555/696
7	68748293/33408	1066015037/33408
8	10326863/1856	88042953/8352
9	253783977/16704	5664272501/16704
10	113829953/2784	2973959761/2784
11	616617891/5568	55253416097/16704
12	9921283537/33408	21086901275/2088
13	13362209531/16704	508886033383/16704
14	71463382173/33408	506516040677/5568
15	191739773753/33408	8994485533345/33408
16	511561441985/33408	3301964087761/4176
17	1368443702359/33408	8561214321183/3712
18	1214746654897/11136	111697968493535/16704

Table II. Coefficients $C(x)$ and $R(x)$ for SAWs on the Sierpinski Carpet with $b=7$, $m=9$ (see Fig. 2b)

n	C_n	ρ_n
1	182/47	182/47
2	528/47	1408/47
3	30807/940	139607/940
4	41501/470	58046/94
5	22913/94	1084481/470
6	610407/940	3792521/470
7	165117/94	12647509/470
8	436017/94	40739336/470
9	465341363/37600	10215742339/37600
10	305460951/9400	1958733547/2350
11	3229577743/37600	18891719643/7520
12	2110315247/9400	35078924529/4700
13	5542013239/9400	205936218759/9400
14	14435239231/9400	119685077599/1880
15	150961289197/37600	1723931566617/9400
16	78439110813/7520	4929142078277/9400
17	1022039468727/37600	56000535076967/37600
18	2649923058101/37600	79060765759227/18800

Table III. Coefficients $C(x)$ and $R(x)$ for SAWs on the Sierpinski Carpet with $b=7$, $m=9$ (see Fig. 2c)

n	C_n	ρ_n
1	117/31	117/31
2	330/31	880/31
3	1871/62	8463/62
4	97519/1240	681024/1240
5	520643/2480	4918187/2480
6	668567/1240	8305914/1240
7	3487859/2480	53491859/2480
8	8865873/2480	83250162/1240
9	11394207/1240	252358531/1240
10	57604051/2480	749189531/1240
11	146674303/2480	4371527287/2480
12	184636936/1240	3143951199/620
13	467332593/1240	17878761053/1240
14	2346766139/2480	10064654037/248
15	2958269782/1240	140437005034/1240
16	296559205293/49600	972229508503/3100
17	372798788797/24800	4278413058889/4960
18	18660653341777/49600	14617377705617/6200

Table IV. Coefficients $C(x)$ and $R(x)$ for SAWs on the Sierpinski Carpet with $b=3$, $m=1$ (see Fig. 2d)

n	C_n	ρ_n
1	42/11	42/11
2	120/11	320/11
3	1379/44	6243/44
4	1825/22	6375/11
5	79169/352	748137/352
6	51695/88	320855/44
7	548621/352	8401085/352
8	1419981/352	6644089/88
9	1857937/176	40923089/176
10	9567527/352	123423015/176
11	198498261/2816	5853951733/2816
12	31817111/176	1069407931/176
13	328062195/704	12354078169/704
14	1677615671/1408	35316758085/704
15	4305919093/1408	200127960733/1408
16	10983364177/1408	281328468717/704
17	3512719205/176	49098876469/44
18	71549402013/1408	1090218120733/352

Table V. Coefficients $C(x)$ and $R(x)$ for SAWs on the Sierpinski Carpet with $b=5$, $m=9$ (see Fig. 2e)

n	C_n	ρ_n
1	210/61	210/61
2	528/61	1408/61
3	5341/244	23877/244
4	12187/244	42537/122
5	57311/488	543671/488
6	64249/244	406639/122
7	589579/976	9274523/976
8	5341807/3904	51032471/1952
9	118677773/3904	274374053/3904
10	26372337/3904	180144509/976
11	59257245/3904	1860446153/3904
12	131654839/3904	2361402615/1952
13	294339305/3904	11832763917/3904
14	653479731/3904	7330081535/976
15	1455378635/3904	71903470743/3904
16	201662325/244	87536531663/1952
17	14326545627/7808	845589313155/7808
18	15844414027/3904	507819935985/1952

Table VI. D log Padé Approximants to the Generating Function $C(x)$ of Lattice 1 (see Fig. 2a)

N	$[N-1/N]$ Pole (residue)	$[N/N]$ Pole (residue)	$[N+1/N]$ Pole (residue)
1	0.504462(−2.00045)	0.286531(−0.64538)	0.590297(−5.64301)
2	0.391173(−1.39713)	0.390144(−1.38656)	0.374306(−1.17795)
3	0.391249(−1.39762)[a]	0.376032(−1.20466)	0.372172(−1.15872)[a]
4	0.378672(−1.25116)	0.384316(−1.39678)	0.376975(−1.21071)
5	0.379938(−1.27478)	0.380444(−1.28710)	0.381133(−1.30742)
6	0.375648(−1.33206)[a]	0.381453(−1.31914)	0.383166(−1.45043)[a]
7	0.381737(−1.33179)	0.381845(−1.33749)	0.381903(−1.34097)
8	0.381985(−1.34676)[a]	0.381771(−1.33386)[a]	0.382164(−1.36035)

[a] Pole present between the origin and 1.15 times the displayed physical singularity.

Table VII. D log Padé Approximants to the Generating Function $C(x)$ of Lattice 2 (see Fig. 2b)

N	$[N-1/N]$ Pole (residue)	$[N/N]$ Pole (residue)	$[N+1/N]$ Pole (residue)
1	0.518173(−2.00654)	0.288759(−0.62312)	0.614410(−6.00257)
2	0.398766(−1.38756)	0.398889(−1.38879)	0.383311(−1.18738)
3	0.398767(−1.38757)	0.385206(−1.21617)	0.381044(−1.16696)[a]
4	0.388028(−1.26442)	0.401714(−1.71960)	0.385832(−1.21469)
5	0.390119(−1.30262)	0.391563(−1.33881)	0.393676(−1.40894)
6	[b]	0.394599(−1.44944)	0.394236(−1.43194)
7	0.394018(−1.42115)	0.395145(−1.47468)[a]	0.393289(−1.39050)
8	0.392080(−1.33469)	0.392933(−1.37415)	0.392594(−1.35627)
9	0.392788(−1.36709)		

[a] Pole present between the origin and 1.15 times the displayed physical singularity.
[b] No poles found.

Table VIII. D log Padé Approximants to the Generating Function $C(x)$ of Lattice 3 (see Fig. 2c)

N	$[N-1/N]$ Pole (residue)	$[N/N]$ Pole (residue)	$[N+1/N]$ Pole (residue)
1	0.535667(−2.02171)	0.296500(−0.61941)	0.660244(−6.83940)
2	0.413119(−1.40583)	0.416343(−1.43752)	0.400173(−1.23052)
3	0.413679(−1.40971)	0.402487(−1.26552)	0.393781(−1.20102)[a]
4	0.405003(−1.30759)	0.419131(−1.80562)	0.398954(−1.21193)[a]
5	0.406465(−1.33310)	0.407015(−1.34569)	0.407537(−1.36002)
6	0.412019(−1.70007)[a]	0.407386(−1.35545)	0.407707(−1.36440)[a]
7	0.407081(−1.34618)[a]	0.410745(−1.41028)[a]	0.405730(−1.30702)
8	0.403917(−1.22779)	0.407317(−1.35853)	0.406235(−1.32419)
9	0.405609(−1.29961)		

[a] Pole present between the origin and 1.15 times the displayed physical singularity.

Table IX. D log Padé Approximants to the Generating Function $C(x)$ of Lattice 4 (see Fig. 2d)

N	$[N-1/N]$ Pole (residue)	$[N/N]$ Pole (residue)	$[N+1/N]$ Pole (residue)
1	0.527397(−2.01370)	0.292779(−0.62058)	0.637951(−6.42010)
2	0.406267(−1.39630)	0.408105(−1.41454)	0.392510(−1.21376)
3	0.406470(−1.39769)	0.394365(−1.24186)	0.388608(−1.18876)[a]
4	0.396640(−1.28095)	[b]	0.391488(−1.19940)[a]
5	0.398105(−1.30734)	0.398751(−1.32269)	0.399576(−1.34676)
6	0.392625(−1.40197)[a]	0.399893(−1.35814)	0.399912(−1.35894)
7	0.399911(−1.35889)	0.399894(−1.35821)	0.399727(−1.35117)
8	0.399466(−1.33782)	0.399308(−1.32835)	0.399825(−1.35503)[a]
9	0.399478(−1.33846)[a]		

[a] Pole present between the origin and 1.15 times the displayed physical singularity.
[b] No poles found.

Table X. D log Padé Approximants to the Generating Function $C(x)$ of Lattice 5 (see Fig. 2e)

N	$[N-1/N]$ Pole (residue)	$[N/N]$ Pole (residue)	$[N+1/N]$ Pole (residue)
1	0.630538(−2.17070)	0.319784(−0.55833)	0.928221(−13.65449)
2	0.475372(−1.47483)	0.487754(−1.58583)	0.459160(−1.25302)
3	0.479259(−1.50061)	0.459042(−1.25143)	0.459152(−1.25293)
4	0.460628(−1.27684)	[b]	0.459343(−1.25512)[a]
5	0.460832(−1.28014)	0.459686(−1.26025)	0.459429(−1.25619)
6	0.450556(−1.03942)	0.451659(−1.07286)	0.454908(−1.16728)
7	0.450273(−1.03146)[a]	0.455877(−1.19422)	0.449109(−1.09320)[a]
8	0.457312(−1.23746)	0.461909(−1.43436)	[b]
9	0.456576(−1.21657)[a]		

[a] Pole present between the origin and 1.15 times the displayed physical singularity.
[b] No poles found.

Table XI. D log Padé Approximants to the Generating Function $R(x)$ of Lattice 1 (see Fig. 2a)

N	$[N-1/N]$ Residue	$[N/N]$ Residue	$[N+1/N]$ Residue
1	2.12619	2.47036	2.57971
2	2.59061	2.51782	2.42387
3	2.44127	2.42389	2.42387
4	2.43830	2.45767	2.45918
5	2.45923	2.45735	2.47263
6	2.47718	2.47577	2.68625[a]
7	2.47674	2.47765	2.47813
8	2.47865	2.47748	

[a] Pole present near the biased critical value $x^* = 1$.

Table XII. D log Padé Approximants to the Generating Function $R(x)$ of Lattice 2 (see Fig. 2b)

N	$[N-1/N]$ Residue	$[N/N]$ Residue	$[N+1/N]$ Residue
1	2.10319	2.45848	2.56858
2	2.57979	2.50550	2.39929
3	2.42080	2.38372	2.39750
4	2.41204	2.42560	2.42138
5	2.42196	2.42363	2.41625
6	2.42020	2.41834	2.41675
7	2.42091	2.42587	2.38206
8	2.41717	2.45791	

Table XIII. D log Padé Approximants to the Generating Function $R(x)$ of Lattice 3 (see Fig. 2c)

N	$[N-1/N]$ Residue	$[N/N]$ Residue	$[N+1/N]$ Residue
1	2.09277	2.45474	2.57123
2	2.58381	2.50813	2.44024
3	2.45054	2.45518	2.43611
4	2.45021	2.49095	2.51890
5	2.52489	2.41479	2.60269
6	2.62315	2.68500	2.71130[a]
7	2.71441[a]	2.68720	2.59847
8	2.62474	2.05370[a]	

[a] Pole present near the biased critical value $x^* = 1$.

Table XIV. D log Padé Approximants to the Generating Function $R(x)$ of Lattice 4 (see Fig. 2d)

N	$[N-1/N]$ Residue	$[N/N]$ Residue	$[N+1/N]$ Residue
1	2.09764	2.45604	2.56705
2	2.57847	2.50448	2.42153
3	2.43562	2.43062	2.42021
4	2.43529	2.46281	2.47382
5	2.47564	2.45286	2.55281
6	2.61425[a]	2.62386[a]	2.58440
7	2.61519[a]	2.68300[a]	2.54631
8	2.59912[a]	2.51948	

[a] Pole present near the biased critical value $x^* = 1$.

Table XV. D log Padé Approximants to the Generating Function $R(x)$ of Lattice 5 (see Fig. 2e)

N	$[N-1/N]$ Residue	$[N/N]$ Residue	$[N+1/N]$ Residue
1	2.02976	2.44424	2.67166
2	2.72107	2.60400	2.59416
3	2.59473	2.60825	2.58140
4	2.58339	2.59370	2.59286
5	2.59288	2.59376	2.60169
6	2.60266	2.58640	0.26210[a]
7	2.35605	1.22496[a]	0.19732[a]
8	2.27807	2.40228	

[a] Pole present near the biased critical value $x^* = 1$.

Table XVI. Critical Parameters and Exponents for SAWs on Sierpinski Carpets Obtained from the 18th-Order Series Expansion, together with Results for the Square Lattice

Lattice	D_f	$\langle q \rangle$	x_c	γ	ν
1	1.975	1.983	0.3818 ± 0.0003	1.338 ± 0.030	0.739 ± 0.007
2	1.896	1.936	0.3933 ± 0.0010	1.36 ± 0.07	0.71 ± 0.10
3	1.896	1.887	0.4058 ± 0.0018	1.30 ± 0.19	0.82 ± 0.09
4	1.893	1.909	0.3997 ± 0.0005	1.35 ± 0.05	0.80 ± 0.06
5	1.723	1.721	0.458 ± 0.005	1.26 ± 0.37	0.7 ± 0.5
Square[a]	2	2	0.3789 ± 0.0003	1.331 ± 0.013	0.744 ± 0.008

[a] Exact values: $\gamma^{(2)} = 1.34375$, $\nu^{(2)} = 0.75$ (ref. 5). Best estimate: $x_c^{(2)} = 0.379052(0)$ (ref. 4).

4. DISCUSSION AND CONCLUSIONS

From Table XVI, it is not possible to order exponents γ and ν against D_f, but the critical fugacity x_c depends monotonically on q, as expected (see Fig. 3). In fact, from Fig. 3, the dependence of x_c on q is approximately linear for this range of D_f.

Table XVI also shows that lattices 1 and 2 have central values estimate $\nu_{\text{SAW}} < \nu^{(2)}$ (exact result for the square lattice). For lattice 2, it is also the trend shown by the last approximants in Table XII. These results do not support previous findings in the literature such as ν_k [Eq. (1)] or the ones obtained from a bond-moving scheme ν_T.[19] Both approaches estimate $\nu_{\text{SAW}} > \nu^{(2)}$ for all families of carpets (see Table XVII).

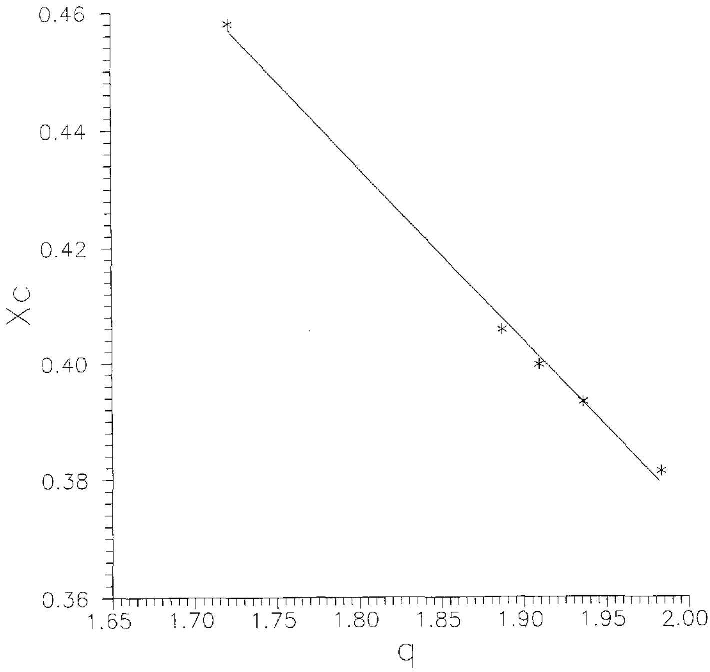

Fig. 3. Critical fugacity versus average number of bonds per site of Sierpinski carpets obtained from the 18th-order series expansion. The result for the square lattice is also included.

Now consider the ν_{SAW} estimates from Table XVI for lattices 3 and 4. While the final results include $\nu^{(2)}$, Tables XIII and XIV of the last approximants suggest that for these lattices the $(2\nu_{\mathrm{SAW}}+1)$ estimates converge to values greater than $(2\nu^{(2)}+1)$.

Table X for the ν_{SAW} estimates of lattice 5 have anomalous highest

Table XVII. End-to-End Distance Exponent ν_{SAW} for SAWs on Sierpinski Carpets

Lattice	ν_{SAW} [a]	ν_k [b]	ν_T [c]
1	0.739 ± 0.007	0.755	0.796
2	0.71 ± 0.10	0.770	0.812
3	0.82 ± 0.09	0.770	0.814
4	0.80 ± 0.06	0.771	0.829
5	0.7 ± 0.5	0.806	0.869

[a] This work.
[b] Ref. 10.
[c] Ref. 16.

Table XVIII. Exponent γ_{SAW} for SAWs on Sierpinski Carpets

Lattice	γ_{SAW} [a]	γ_k [b]
1	1.338 ± 0.030	1.510
2	1.36 ± 0.07	1.540
3	1.30 ± 0.19	1.540
4	1.35 ± 0.05	1.542
5	1.26 ± 0.37	1.612

[a] This work.
[b] Ref. 17.

order approximants indicating a possible change in the end-to-end distance behavior. As consequence, the final results for the exponents of this lattice have poor accuracy and it is not possible to draw any conclusion from them.

The results for the end-to-end distance exponent of lattices 3 and 4 can be understood if we consider their initiators (Figs. 2c and 2d, respectively). As we iterate them, the fractal lattices thus obtained leave narrow corridors to embed the SAWs. They show a tendency to stretch in order to survive, leading to $\nu_{SAW} > \nu^{(2)}$ (or $D_{SAW} = 1/\nu_{SAW} < 1/\nu^{(2)}$) for carpets with high lacunarity.

The new behavior $\nu_{SAW} < \nu^{(2)}$ for lattices 1 and 2 can also be understood if we consider their initiators (Figs. 2a and 2b), which have lacunas spread over the square lattice. These lacunas, as prohibited regions for the growing SAW, act as repelling centers that confine the walk. Therefore, there is an enhancement of the weight of twisted walks among the statistically relevant configurations of SAWs, leading to a smaller ν_{SAW} (or greater D_{SAW}) as compared with the square lattice.

From Tables XVI and XVII, our results indicate that, contrary to the previous findings in the literature such as ν_K and ν_T, lacunarity plays an important role in the universality classes.

Another extension for fractals based on the Flory approach for Euclidean lattices[20] is

$$\gamma = 6/(2 + D_f) \tag{9}$$

which also leads to results in disagreement with ours (see Table XVIII).

Our results indicate that the γ_{SAW} behavior does not follow that of ν_{SAW} as suggested by Eqs. (1) and (9). For example, the central values of our estimates for lattices 2 and 4 suggest that they have near values of γ_{SAW}, while lattice 4 has ν_{SAW} greater than that of lattice 2.

In summary, the series expansion method, based on an exact graph counting technique for connected graphs on self-similar fractals, is a powerful method that provides results for critical parameters and exponents for the SAW problem on infinitely ramified fractals.

The results presented here were used to analyze the role of geometrical factors (e.g., average coordination number and lacunarity) on the critical parameters and exponents. The critical fugacity was obtained with good accuracy for carpets and varies linearly with the average coordination numbers of these fractal lattices. We also obtained that, contrary to previous estimates in the literature, for low lacunar fractals we may have $\nu_{\mathrm{SAW}}(\mathrm{fractal}) < \nu_{\mathrm{SAW}}(d)$ for the SAW problem on a d-dimensional Euclidean lattice that embeds the fractal. This result is analogous to the random walk problem, although here $D_{\mathrm{SAW}} < D_f$ due to the self-repelling condition.

Due to the relatively low-order series obtained so far, it was only possible to draw qualitative conclusions for the exponents. On the other hand, by increasing the order of the series, this method can also provide very accurate results for the critical exponents of the SAW problem on carpets.

Our method of graph counting also allows calculation of geometrical parameters of the fractal lattices in the $l \to \infty$ stage, such as lacunarity, which has been calculated so far in the literature only for the first stages of the carpets. Accurate measurements of this geometrical factor for the carpets and more accurate estimates of critical exponents using this method may lead to a quantitative description of universality classes of the SAW problem on these fractals. Work along these lines is in progress.

APPENDIX

Consider a particular n-step SAW and the minimal stage l_0 that embeds it. The number of ways of embedding the SAW at stage $l > l_0$ is

$$G(l) = (b^2 - m)\, G(l-1) + H(l-1) \tag{A.1}$$

with $H(l-1)$ the number of configurations that cross the intersections of the $(b^2 - m)$ reproductions of the $(l-1)$ stage in the l stage.

Contributions to $H(l-1)$ come from configurations that cross just one intersection $[H_1(l-1)]$ or more than one intersection $[H_2(l-1)]$ of the $(l-1)$-stage reproductions.

Now, consider all possible types of partitionings i of the SAW across one such intersection [this means, for instance, that the SAW crosses one boundary of one $(l-1)$-stage reproduction at the ith step].

The contribution of partitioning i to $H_1(l-1)$ is given by $H_1^{(i)}(l-1)$.

As the SAW necessarily crosses one border of the $(l-1)$-lattice stage and there are b reproductions of the $(l-2)$-stage at each border of the $(l-1)$-stage (see Fig. 1), using the same reasonings that led to (A.1), we find

$$H_1^{(i)}(l-1) = bH_1^{(i)}(l-2) + A_1^{(i)} \tag{A.2}$$

with constant $A_1^{(i)}$ representing the number of configurations that also cross the neighboring $(l-2)$-stage reproductions at this border of the $(l-1)$ stage. As the original SAW involves regions up to the l_0-stage spatial scale, the constant $A_1^{(i)}$ is obtained just considering neighboring l_0-stage reproductions.

Iterating (A.2) up to l_0, we find

$$H_1^{(i)}(l-1) = b^{l-1-l_0} H_1^{(i)}(l_0) + B_1^{(i)} = b^{l-1} C_1^{(i)} + D_1^{(i)} \tag{A.3}$$

with constants $C_1^{(i)}$ and $D_1^{(i)}$ depending on the properties of the SAW at the l_0 stage of the lattice and on the scaling factor b.

Now, consider all possible types of partitionings of the SAW across two or more intersections of neighboring $(l-1)$-stage reproductions. For each partitioning i, $H_2^{(i)}(l-1) = 1$.

All these possible partitionings involve spatial scales that are embedded in neighboring l_0-stage reproductions. This means that

$$H_2^{(i)}(l-1) = H_2^{(i)}(l_0) = 1 \tag{A.4}$$

Adding (A.3) and (A.4) for all possible partitionings and intersections gives

$$H(l-1) = H_1(l-1) + H_2(l-2) = C_1 b^{l-1} + C_2 \tag{A.5}$$

with

$$H_1(l-1) = \sum_{(i)} H_1^{(i)}(l-1) \qquad \text{and} \qquad H_2(l-1) = \sum_{(i)} H_2^{(i)}(l-1)$$

ACKNOWLEDGMENTS

We are grateful to S. L. A. de Queiroz for a critical reading of the manuscript. This work was supported by Brazilian agencies CNPq and SCT/PR.

REFERENCES

1. P. J. Flory, in *Principles of Polymer Chemistry* (Cornell University Press, Ithaca, New York, 1971).
2. P. G. de Gennes, in *Scaling Concepts in Polymer Physics* (Cornell University Press, Ithaca, New York, 1979).

3. D. C. Rapaport, *J. Phys. A* **18**:L201 (1985).
4. A. J. Guttmann, *J. Phys. A* **20**:1839 (1987).
5. B. Nienhuis, *Phys. Rev. Lett.* **49**:1062 (1982); *J. Stat. Phys.* **34**:731 (1984).
6. J. C. Le Guillou and J. Zinn-Justin, *J. Phys. Lett.* (Paris) **46**:L137 (1985).
7. B. B. Mandelbrot, in *The Fractal Geometry of Nature* (Freeman, San Francisco, 1982).
8. R. Rammal, G. Toulouse, and J. Vannimenus, *J. Phys.* (Paris) **45**:389 (1984).
9. S. B. Lee, H. Nakanishi, and Y. Kim, *Phys. Rev. B* **39**:9561 (1989).
10. K. Kremer, *Z. Phys. B* **45**:149 (1981).
11. R. Dekeyser, A. Maritan, and A. L. Stella, *Phys. Rev. Lett.* **58**:1758 (1987).
12. A. Aharony and A. B. Harris, *J. Stat. Phys.* **54**:1091 (1980).
13. K. Yao and G. Zhuang, *J. Phys. A* **23**:L1259 (1990).
14. Fábio D. A. A. Reis and R. Riera, *Phys. Rev. A* **45**:2628 (1992).
15. Y. Gefen, A. Aharony, and B. B. Mamdelbrot, *J. Phys. A* **17**:1277 (1984).
16. Y. Taguchi, *J. Phys. A* **20**:6611 (1987).
17. G. A. Baker, Jr., in *Essentials of Padé Approximants* (Academic Press, New York, 1975).
18. G. A. Baker, Jr., and G. Morris, in *Encyclopedia of Mathematics and its Applications*, Vol. 13 (Cambridge University Press, Cambridge, 1981).
19. Y. Taguchi, *J. Phys. A* **21**:1929 (1988).
20. L. Pietronero and L. Peliti, *Phys. Rev. Lett.* **55**:1479 (1985).